Classification of common human diseases derived from shared genetic and environmental determinants

Kanix Wang[1,2], Hallie Gaitsch[2], Hoifung Poon[3], Nancy J Cox[4] & Andrey Rzhetsky[2,5]

In this study, we used insurance claims for over one-third of the entire US population to create a subset of 128,989 families (481,657 unique individuals). We then used these data to (i) estimate the heritability and familial environmental patterns of 149 diseases and (ii) infer the genetic and environmental correlations for disease pairs from a set of 29 complex diseases. The majority (52 of 65) of our study's heritability estimates matched earlier reports, and 84 of our estimates appear to have been obtained for the first time. We used correlation matrices to compute environmental and genetic disease classifications and corresponding reliability measures. Among unexpected observations, we found that migraine, typically classified as a disease of the central nervous system, appeared to be most genetically similar to irritable bowel syndrome and most environmentally similar to cystitis and urethritis, all of which are inflammatory diseases.

Disease classifications (nosologies) are used ubiquitously in academic medicine, human genetics, the health industry, and economics. Much like any library's content catalog, disease taxonomies strive to group together similar entities for ease of access and analysis. Initially, many of these groupings were largely arbitrary—often guided by topographical, anatomical, or even cultural similarities[1,2].

Historically, changes in these groupings have reflected a progression toward etiologic, common-cause disease classifications.

The evolution of nosologies has closely paralleled the evolution of methods designed for reconstruction of the universal tree of life. Approaches to species classifications were initially subjective or heuristic[3–7] and made without any hint of the common-origin interpretation, using only a small subset of all the visible morphological features of any given organism. These early phylogenetic methods were followed by the use of maximum-parsimony methods, explicitly minimizing the number of differences between proximal taxonomy leaves. Most recent arrivals to phylogenetics are statistical tree-making methods[8], which infer taxonomies from very large data sets using explicit stochastic models of diverging organism traits during speciation.

In this study, we synthesized a synergy of the analytical methods developed for phylogenetic analysis with those established in dissecting the heritable and environmental components of human disease. The main premise of our analysis was that etiological disease taxonomy can and should be constructed using the explicit and objective genetic and environmental correlations between diseases[9]. Such a classification would maximize genetic and/or environmental disease similarities that have clustered together and would generate the closest yet approximation to the common-cause nosology.

Our study used a data set summarizing health information for more than one-third of the US population, including more than 40 million families. The most informative subset of these, 481,657 unique individuals grouped into 128,989 families, was chosen for in-depth genetic analysis. In this study, we focused on estimating heritability and environmental and genetic correlations between common diseases that were unambiguously coded in the insurance claims. Doing so, we were unable to analyze quantitative traits, which are not represented in insurance claims.

A trait's narrow-sense heritability is defined as the ratio of its additive genetic variance[10,11] to its total phenotypic variance (see ref. 12). The environment-related counterpart to narrow-sense heritability is, consequently, the ratio of the environment-related variance (unique for an individual, shared by siblings, parents, or the entire family) to the total disease-specific phenotypic variance. The environment-related variance portion of this ratio can be called preventability because it indicates the putative efficacy of interventions via changing environmental conditions.

RESULTS

Data

Our data set was generated by subsampling from a very large collection of families represented in a compilation of insurance claims from Truven MarketScan. By definition, the data set included only information about insured families, and it is therefore slightly biased toward more affluent urban populations (**Fig. 1a**). The largest families, as well as the majority of all families, were urban (**Fig. 1a,b**), with the overall urban population share slightly higher than the 80.7% reported by the US Census Bureau (see URLs). It is therefore unlikely that our heritability and genetic correlation estimates were affected by the sampling of families from rural areas, where average relatedness of individuals in the same county is potentially higher than the country average.

[1]Committee on Genetics, Genomics, and Systems Biology, University of Chicago, Chicago, Illinois, USA. [2]Institute of Genomics and Systems Biology, University of Chicago, Chicago, Illinois, USA. [3]Microsoft Research, Redmond, Washington, USA. [4]Vanderbilt Genetics Institute, Vanderbilt University, School of Medicine, Nashville, Tennessee, USA. [5]Department of Medicine, Department of Human Genetics, and Computation Institute, University of Chicago, Chicago, Illinois, USA. Correspondence should be addressed to A.R. (andrey.rzhetsky@uchicago.edu).

The need to focus on a subset of families out of the total 40 million families was two-pronged. First, computational tractability demanded that we significantly restrict the sample: the bivariate analysis of common diseases can become impractical if the sample is too large. Second, in insurance claims, the data of parents and their children are linked for a limited time (**Fig. 1c**). Typically, US children can only be covered by their parent's health insurance until the age of 25. As a consequence, the apparent disease prevalence in offspring is much lower than in their parents. Therefore, we focused on a set of 128,989 families in which both parents and children were 'visible' for the longest time interval, but no less than 6 years. No individual in the data was visible for more than 10 years. The methods we used in this study are robust to age-dependent prevalence assuming the same liability with age-dependent threshold (Online Methods). We concede that assuming that early-onset and late-onset diseases have the same underlying liability is a limitation of this method; clearly, in principle these disease versions could represent fundamentally different conditions.

Model selection

We started our analysis with a systematic comparison of those mathematical models most likely to describe the structure of our data set families' phenotypic variance (**Fig. 1d** and Online Methods; DIC stands for deviance information criterion, commonly used in Bayesian model selection[13]). The best model included shared couple (parents) environment, shared sibling environment, and additive genetics (see the *GCS* model in **Fig. 1d**). The second best model dropped the shared sibling environment component, *S* (**Fig. 1d**). We then used the *GCS* and *GC* models (whichever fit data best) to estimate liability-scale heritability and its environmental counterpart ('preventability') for 149 common diseases (**Fig. 1e** and **Supplementary Fig. 1**; disease abbreviations are given in **Supplementary Table 1**).

Estimates of liability-scale heritability

We estimated the narrow-sense heritability for 149 of the most common diseases present in the insurance claim data set (see **Fig. 1e** and the 30 most prevalent diseases in **Table 1**). To the best of our knowledge, these estimates were obtained for the majority of diseases for the first time in our study: 84 of 149 estimates (56%) are new. These putative first-time estimates are marked with asterisks in **Figure 1e** (see details in the Online Methods and **Supplementary Table 2**).

Our liability-scale heritability estimates spanned a wide range of values, from 0.924 (autism) to 0.038 (lipoma). The apparent correlation between our estimates for heritability and disease prevalence turned out to be significantly negative (**Fig. 1f**): the estimated linear regression slope was −1.20 (standard error (se) = 0.455, $P = 0.00915$), with Pearson's $r = -0.212$ (95% confidence interval (CI) = −0.36, −0.05) and $P = 0.00915$.

Of the 65 diseases in our disease set with previously published heritability estimates, 52 of our estimates agreed with the published estimates within the 95% CI (**Fig. 1g** and **Supplementary Table 3**; specifically, the 95% CIs of the two heritability estimates for the same condition overlapped; phenotypes that were discordant with our estimates are indicated by bold typeface in **Supplementary Table 3**). The published and new estimates were highly correlated ($r = 0.571$, CI = 0.379, 0.715, $P = 6.902 \times 10^{-7}$, linear slope = 0.4975, se = 0.0902, $P = 6.90 \times 10^{-7}$). Furthermore, the error bars for the new heritability estimates (**Fig. 1g**) are predominantly much narrower than those published. The mean values of our heritability estimates are, on average, slightly lower than previously published values, as can be seen by comparing the dotted regression line (slope = 0.5) with the

blue line (slope = 1) in **Figure 1g**. Various possible sources of this trend have been enumerated below.

According to common genetics wisdom, diseases with early onset tend to have higher heritability. This assumption was tested by using heritability and onset estimates of our 149 chosen diseases (Online Methods and **Supplementary Fig. 2a,b**). The correlation between the age of onset and disease heritability appears negative for a subset of diseases, including those currently categorized as neuropsychiatric, neoplastic, metabolic, ophthalmologic, and central nervous system diseases. For diseases with strong immune system components, such as autoimmune and infectious diseases, the estimated correlation between heritability and disease onset was positive (**Supplementary Fig. 2b**). When combined, the heritability estimates for all diseases, contrary to the common wisdom, showed no linear correlation with age of disease onset.

Our analysis also provided estimates of the environmental counterparts of heritability: unique-environment, common-couple, and common-sibling preventability (**Supplementary Fig. 1a–c**). The common-couple preventability estimates range from 0 (autism) to 0.46 (photo dermatitis); the corresponding common-sibling estimates tend to be smaller but can be as large as 0.29 (sepsis). The estimates for unique-environment preventability tend to be the largest: in our data set, estimates ranged from 0.03 (eye infection) to 0.842 (diseases associated with damages to rectum and anus). For example, the largest preventability estimate for migraine is for unique environment (0.534), followed by common-couple preventability 0.11 and negligible common-sibling preventability. Similarly, for sleep disorders, preventability estimates were 0.269, 0.22, and 0.15 for unique, couple, and sibling preventability, respectively.

Genetic and environmental correlations

Our analysis of pairwise disease correlations focused on 29 diseases, all pairs of which were well represented in both the children and parents of our data set (**Supplementary Table 1**). We estimated genetic and environmental correlations across all pairs of these 29 diseases (**Fig. 2a–d** and **Supplementary Table 4**)[14]. The majority of correlation values in our analysis differed significantly from zero (the null hypothesis $r = 0$) at a 1% false discovery rate (Online Methods)[15]. On average, genetic correlations between diseases tended to be stronger than their corresponding environmental correlations (**Fig. 2b,c**). However, for the majority of neuropsychiatric disease pairs, the environmental correlations are nearly as strong as the genetic correlations. In some cases, such as for the substance abuse and schizophrenia disease pair, the environmental correlation is stronger than the genetic correlation, and nearly equal for other disease pairs, such as schizophrenia and bipolar disorder. This observation is consistent with an earlier finding of nearly equal amounts of shared genetic and environmental effects between schizophrenia and bipolar disorder[16].

The environmental correlation distribution has a longer positive tail than the more symmetric genetic correlation distribution (**Fig. 2c**). Genetic and environmental correlations for the same disease pair were themselves positively correlated, and genetic correlations were also positively correlated with phenotypic correlations (**Supplementary Fig. 3a,b**).

In a few cases, the direction of a correlation was reversed between genetic and environmental components (**Fig. 2a**, colored rectangles). The corresponding Bayesian posterior probabilities for the significance of this sign difference are given in the figure legend. These cases were particularly unexpected, as they indicate hypothetical scenarios in which genetic and environmental factors act antagonistically in
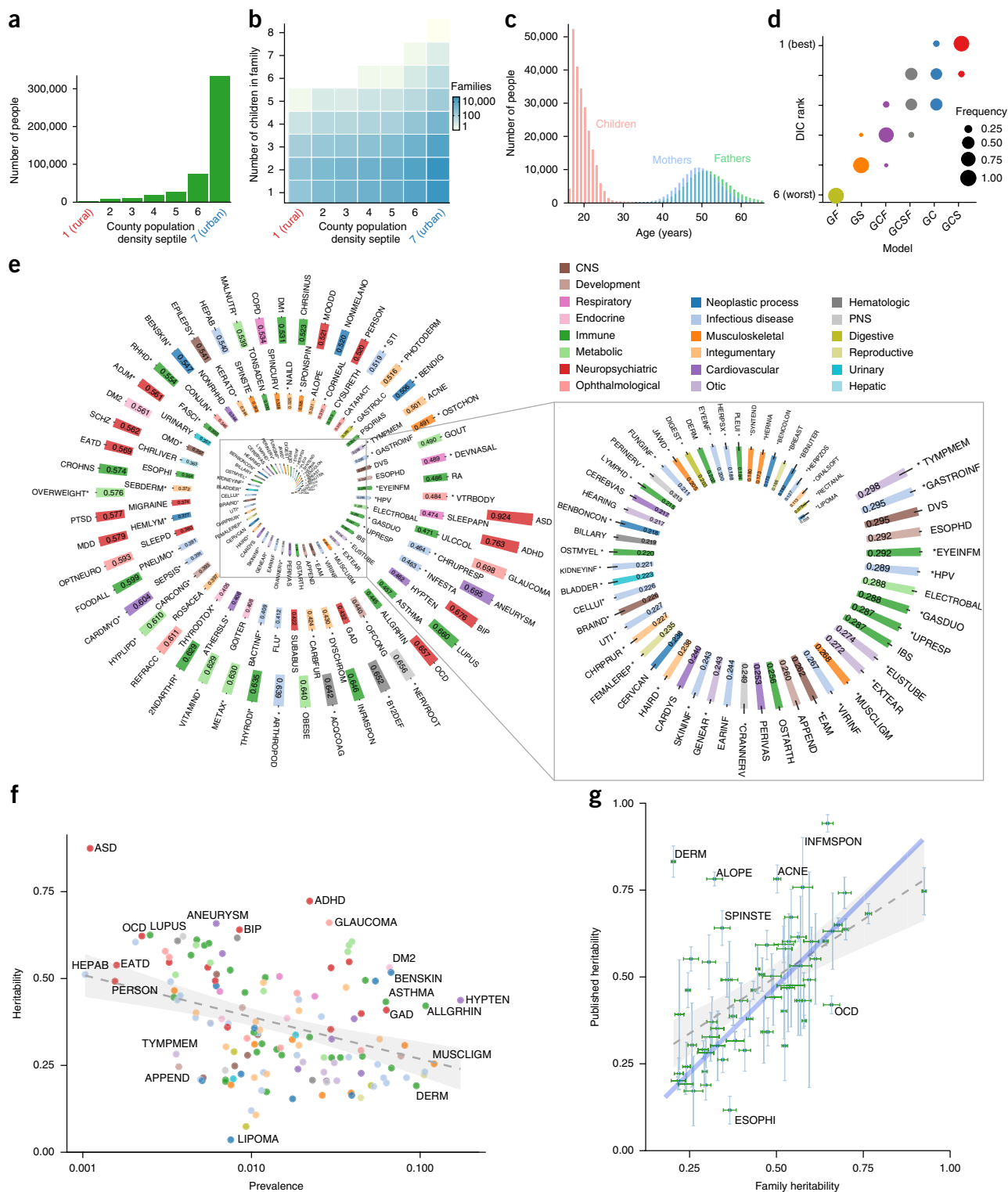
Figure 1 Information on study population, results of model selection, and analysis of heritability of 149 diseases. (**a**) Distribution of the study population across population density septiles; septile 1 corresponds to the most rural counties and septile 7 corresponds to the most urban septile. (**b**) Number of children in a family as a function of population density septile; septile notations are the same as in **a**. (**c**) Parent/child age distribution in studied families. (**d**) Model selection results, using univariate models *GF*, *GS*, *GCF*, *GCSF*, *GC*, and *GCS*, where *G* stands for additive genetics, *F* for common family environment, *S* for common sibling environment, and *C* for environment common for parental couples; the plot shows the frequency of the corresponding model becoming the 'best' (rank 1) as compared by deviance information criterion (DIC), second best (rank 2), and so on; the *GCS* model wins in the majority of cases. (**e**) Disease heritability estimates with 1 s.d. Heritability estimates that appear to be measured for the first time are marked with an asterisk; heritability values are sorted in decreasing order; color of the bar indicates biological system associated with the disease; disease acronyms are defined in **Supplementary Tables 1** and **2**. (**f**) Estimates of disease heritability values against estimates of disease prevalence. The linear correlation is significantly negative, Pearson's *r* = −0.212 (95% CI = −0.36, −0.05), and *P* = 0.00915. (**g**) Comparison of our estimates of heritability with previously published estimates; see **Supplementary Table 3** for detailed numbers.
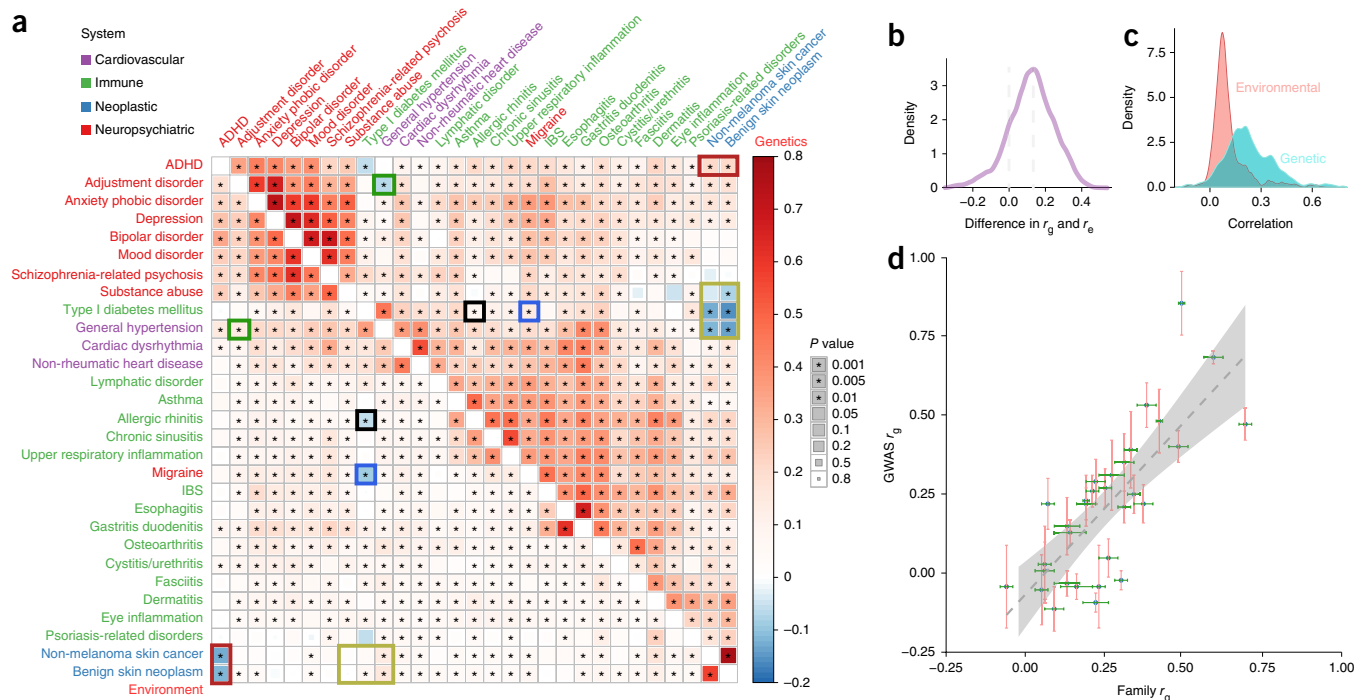
a

Figure 2 Genetic and environmental correlations between diseases. (**a**) Matrix of pairwise genetic correlations (top half) and corresponding environmental interactions (bottom half) colored by sign and magnitude. The disease color labels indicate biological systems associated; the size of the squares indicates statistical significance. Cells with asterisks indicate pairwise interactions that remained significant at a false discovery rate of 1% (ref. 15). The colored boxes within the matrix indicate opposite-sign correlation values for the same pair of diseases. Posterior probabilities of two correlation values (genetic and environmental) for the same pair of diseases having the same sign were 1.869×10^{-14} (ADHD and benign skin neoplasm), 3.376×10^{-14} (ADHD and non-melanoma skin cancer), 4.523×10^{-9} (adjustment disorder and general hypertension), 8.715×10^{-4} (migraine and type 1 diabetes mellitus), 9.251×10^{-5} (benign skin neoplasm and type 1 diabetes mellitus), 6.401×10^{-33} (benign skin neoplasm and general hypertension), 3.712×10^{-17} (non-melanoma skin cancer and general hypertension), 3.933×10^{-4} (allergic rhinitis and type 1 diabetes mellitus). (**b**) Distribution of (genetic correlation – environmental correlation) values for the same pairs of diseases. (**c**) Individual distributions of genetic and environmental correlations superimposed on the same plot. (**d**) Comparison of our family-based estimates of genetic correlations between diseases with previously published GWAS-based values; the complete data on values and references are provided in **Supplementary Table 5**. Linear fit with a slope of 1.08 (s.e.m. = 0.167) is indicated by the dotted line.

determining a phenotypic path bifurcated between two apparently unrelated diseases.

On average, family-based estimates of genetic correlations obtained in our study have much narrower error bars (with a few exceptions) than earlier genome-wide association study (GWAS) estimates (**Fig. 2d** and **Supplementary Table 5**) mostly owing to the very large sample size of our data set. It is noteworthy that genetic correlations obtained by two different methods agree so well. GWAS genetic correlations and family study genetic correlations estimate different quantities: family studies estimate the correlation of the total genetic variation (both rare and common), whereas genetic correlations, estimated using SNPs, are based on genotyped and imputed common SNPs, which are only a subset of the total genetic variation. Essentially, our data suggest that family-based estimates of genetic correlations reflect predominantly common variants.

The absolute values of genetic correlations are high for several common conditions across all the diseases that we analyzed (for example, asthma, allergic rhinitis, osteoarthritis, and dermatitis). This result is surprising, as it suggests that the most prevalent complex diseases share a considerable amount of predisposing variation, even across apparently dissimilar diseases. Human genetic variation associated with common diseases appears highly pleiotropic or even 'omnigenic' (ref. 17).

To get a baseline of the expectedness (or unexpectedness) of observed patterns in genetic and environmental correlations, we used the International Classification of Diseases version 9 (ICD-9; see URLs and **Supplementary Fig. 4**, left). On the basis of the ICD-9 taxonomy, genetic and environmental correlations for migraine are surprising. As migraine is clearly associated with the central nervous system, one would expect that its etiology is most similar to those of other neuropsychiatric conditions. For example, "mental disorders" (codes 290–319 in the ICD-9 taxonomy) have a sister group of "diseases of central nervous system and sensory organs" (codes 320–389), containing both migraine and eye inflammation. However, in our analysis of its genetic and environmental correlations, migraine is not similar to other nervous system diseases. Rather, it is much closer to immune system diseases, such as irritable bowel syndrome (IBS) in the genetic correlation space and to cystitis/urethritis in the environmental correlation space (**Supplementary Fig. 5**). These findings suggest that migraine is associated with general, not nervous-system-specific, inflammatory processes and can possibly be mitigated with some of the treatments that have been developed for inflammatory diseases.

Inferring nosologies from correlations

Relationships among diseases are unlikely to be appropriately described with a tree-like structure commonly used in disease classifications. As we show with our data, genetic and environmental factors suggest partially incompatible disease classifications. In addition, the tree-like structures are implicitly associated with evolving entities

Table 1 Disease prevalence and heritability estimates for the 30 most prevalent diseases in our study

Disease	Prevalence	h^2	h^2 s.d.
Cardiac dysrhythmia	0.045	0.240	0.011
General hypertension	0.173	0.462	0.009
Esophageal disease	0.077	0.292	0.008
Functional digestive disorder	0.051	0.203	0.009
Type II diabetes mellitus	0.066	0.561	0.010
Allergic rhinitis	0.108	0.445	0.006
Asthma	0.063	0.457	0.008
Atopic contact dermatitis	0.095	0.202	0.006
Chronic sinusitis	0.047	0.523	0.008
Eye inflammation	0.045	0.292	0.009
Osteoarthritis	0.068	0.256	0.012
Cellulitis	0.061	0.226	0.007
Ear infection	0.106	0.244	0.007
Eye infection	0.053	0.200	0.009
Fungal infection	0.063	0.211	0.007
UTI	0.083	0.227	0.007
Viral warts HPV	0.038	0.289	0.009
Acne	0.036	0.501	0.010
Keratosis	0.058	0.344	0.015
General spondylosis spine disorder	0.081	0.325	0.008
Muscle ligament disorder	0.121	0.268	0.006
Synovium tendon bursa disorder	0.039	0.180	0.009
Benign colon neoplasm	0.039	0.173	0.019
Benign skin neoplasm	0.067	0.547	0.007
Non-melanoma skin cancer	0.054	0.520	0.008
Anxiety phobic disorder	0.063	0.432	0.007
Depression	0.038	0.579	0.006
Substance abuse	0.045	0.422	0.010
Breast disorder	0.044	0.166	0.010
Disease of the female reproductive organs	0.105	0.235	0.009

with common origin. Tree clustering of diseases should therefore be interpreted with caution because evolutionary relationships do not apply to human diseases.

We use automatically generated classifications (**Supplementary Fig. 5**) as a logically consistent way to visualize and examine all the similarities between all disease pairs simultaneously. To do so, we transform the genetic and environmental correlations shown in **Figure 2a** into distances and then infer objective genetic and environmental disease classifications from those distances. We chose to use the simplest (1 − correlation) distance transformation. The distance-matrix method we used[18] for this purpose is designed to identify the classification topology that approximates the distance matrix the closest, so that the length of the shortest path connecting two classification leaves closely approximates distance in the input matrix. By repeatedly sampling distances from their posterior distribution, one can compute a tree from the resampled distances each time, counting the percentage of times each disease grouping occurs in the resampled trees[19–21] (**Supplementary Fig. 5a,b**). The distances between diseases in a classification are meaningful. For example, two diseases connected with shorter branches are more tightly correlated and more similar genetically and/or environmentally than two diseases connected with very long branches. When a disease group is associated with a reliability number of 100, it means that this particular disease partition was replicated in all trees. In other words, the bootstrap-like numbers[19–21] indicate the statistical reliability of the classification (Online Methods).

In this analysis, the bootstrap-like measures identified a number of remarkably stable disease clusters present in both genetic and environmental trees (**Supplementary Fig. 5**, clusters 1–6). We used the ICD-9 disease taxonomy (**Supplementary Fig. 4**, left) as a baseline to identify disease groupings that are expected (based on ICD-9 classification) and those that are unexpected (defiant of ICD-9 classification, but statistically significant; **Supplementary Fig. 5a,b**, green and yellow highlights, respectively). Many of the stable disease groups (with high bootstrap-like numbers) lie within the traditional view of disease similarity. However, many stable clusters defy the currently established nosology. For example, type 1 diabetes groups with general hypertension (support of 96 and 100 in the environmental and genetic classifications, respectively)—these two diseases are not typically thought to be closely related (see URLs and **Supplementary Fig. 4**). Previously, and collinearly with our results, Farh et al.[22] reported high genetic correlations between type 1 diabetes and other autoimmune diseases.

Migraine in both inferred environmental and genetic classifications appears to be genetically similar to inflammatory diseases such as IBS[23]. However, in the ICD-9 taxonomy (see URLs), migraine is placed together with eye inflammation, in the cluster of diseases of the central nervous system and sensory organs. In our study's genetic tree, eye inflammation is far away from migraine, but is grouped with dermatitis. In the environmental classification, migraine is the closest to inflammations associated with infections cystitis and urethritis; eye inflammation is weakly grouped with the cluster of migraine–cystitis/urethritis. This suggests that migraine etiology is closely associated with immune system function and that the established disease taxonomy needs revision. In a recent study, Gormley et al.[23] also challenged the proximity of migraine to mental disorders; their results were consistent with a vascular etiology of migraine, but while discussing migraine Gormley et al.[23] did not mention IBS or other inflammatory diseases. Here we analyzed migraine phenotypes combining migraine with and without aura. Our data allow distinguishing between these two versions of the disease; therefore, this analysis can be performed with finer disease subdivisions, albeit at the cost of reduced sample size.

Neuropsychiatric diseases stayed in the same stable cluster in both taxonomies (**Supplementary Fig. 4**)[24]. However, within the cluster, disease groupings varied considerably. In our genetic classification, depression was significantly grouped with anxiety. This is in contrast to the ICD-9 taxonomy, which places depression together with mood and bipolar disorders. In our environmental classification, schizophrenia is significantly closer to bipolar and mood disorders than to depression, again contrary to ICD-9.

As expected, a classification computed from complete phenotypic correlations represents a compromise between genetic-only and environmental-only classifications (**Supplementary Fig. 4**, right).

DISCUSSION

We conducted a very large-scale, family-based, phenotypic-variance analysis of numerous complex diseases. Methodologically, our work is indebted to the work of Lichtenstein et al.[16] and Xia et al.[25] in considering genetic data for nosology inference[16] and careful model selection[25]. It has been long suspected that complex diseases have numerous predisposing factors, both in the genetic and environmental realms. For the first time, we were able to compare the contribution of environmental and genetic determinants to the phenotypic variances and covariances of a broad range of diseases, and transform these covariances into estimates of disease classifications.

Our study contributes to a series of influential, interlinked probes into complex disease heritability and cross-disease genetic correlations[24,26–29]. For example, Munoz et al.[30] studied 12 complex human

diseases using 502,682 participants and family histories of disease in 1.5 million individuals. As our data set provides rich phenotypic information for a very large population, we were able to analyze both the heritability and preventability of a collection of diseases (149), an order of magnitude larger than has been previously done, using data for a comparable number of individuals. Furthermore, the statistical power associated with this broad and complex sample provided a new opportunity to contrast genetic correlation estimates from family data with estimates that have been made using DNA variants. Confirming previous findings[29,31], we observed a near-linear relationship between total phenotypic and family-based genetic correlations with a proportionality constant of 1.150 (se = 0.035, $P < 2 \times 10^{-16}$; **Supplementary Fig. 3**). With a much smaller standard error, our ratio estimate is within the confidence intervals of published results[29,31]. These results suggest that the largest part of genetic correlation between complex diseases is associated with common variants captured by SNP genotyping.

As is true for most observational studies, there are several possible sources of bias. Family studies based on closely related individuals may inflate narrow-sense heritability estimates owing to unaccounted for effects of shared environment, maternal influences, or epistatic interactions of genetic variants[32,33]. In agreement with previous findings regarding the significance of shared environmental effects[25,30,34], our study provided first-time or updated heritability estimates for 149 diseases. On average, our heritability estimates were lower than those reported by twin/family studies by a factor of 0.90. Thus, we conclude that SNP-based heritability estimates explain, on average, 49% of our family-based heritability estimates, a 13% increase from previous estimates (**Supplementary Table 6**). Because of the differences in model selection procedures, agreement between our estimates and previously reported results on environmental effects is harder to ascertain[32]. As articulated by Zuk *et al.*[33], one of the major sources of bias in estimates of heritability is associated with the choice of mathematical model, as narrow-sense heritability, by definition, does not account for potential deviations from a genetic additive model. The insurance data describe, at best, 54.7 to 69.7% of the US population, depending on age group (see URLs), so a considerable lower-income stratum of US society is not represented in this data set. Data from insurance claims do not include ethnicity and race; therefore, we were unable to explicitly adjust for these confounders. Another contribution to the estimate bias can be attributed to assortative mating, as the US population is stratified by ethnicity, income, and geography, with all of these factors contributing to assortative marriages.

As would be expected from the age distribution differences in our sample, parental disease prevalence tends to exceed prevalences for the same diseases in their children. This trend would be especially pronounced for late-onset conditions, such as Parkinson's disease and prostate cancer (**Supplementary Table 1**). We accounted for this by modeling age-related increase in disease liability with an age-specific, fixed-effect coefficient in our mixed-effect linear model. (See the Online Methods and **Supplementary Fig. 6** for estimates of dependence of disease liability on age of patient for several late-onset conditions.) Note that this type of modeling only accounts for mean differences in liability between age groups, but not differences in heritability between age groups. If the late-onset and early-onset varieties of the same disease were indeed shown to have distinct etiologies, their heritability values would have to be estimated separately[35].

While ethnicity is not recorded in the US insurance claims, it can be imputed. For example, according to the US Centers for Disease Control and Prevention[36], sickle cell disease (SCD) affects, on average, one out of every 365 African Americans; the incidence rate of SCD

in African Americans is about 88 times higher than in the rest of the US population. The incidence rate of SCD in our database is 2.85523×10^{-4} versus 3.23891×10^{-4} in the nation on average. Given that the US African-American population is 12.2% of the total (see URLs), African-American patients appear to be represented in our data at 10.6% (about 13% lower than the average across the United States). Given the very large sample size, the ethnic diversity of our data set should be a reasonable representation of the multiethnic composition of the US insured population.

When computed solely from genetic information, "genetic correlation is immune to environmental confounding but is subject to genetic confounding" (ref. 24). In the case of family-based analyses, environmental confounding is an issue researchers might address with an appropriate mathematical model of genetic and environmental factors working in consort. Unfortunately, the appropriate model is unknown, and interpretation of results is therefore conditional on the assumptions of a rather simple, additive genetic and additive environmental model—a model that is used in most studies for lack of a better (experimentally grounded) alternative. Another conceivable caveat is related to possible biases in the sampling of affected individuals[24]. Finally, our results reflect the medical coding of disease in the healthcare system rather than research-quality disease diagnoses. Extensive study of the correspondence in results of genetic association studies conducted with research diagnoses and those conducted using diagnoses from electronic health records have demonstrated good concordance for large association studies[37].

The study of Lichtenstein *et al.*[16] discussed the difficulties and ambiguities associated with changing uncertain diagnoses ("patients with one diagnosis sometimes evolve into the other diagnosis"), and, to a large extent, their discussion and hedging apply here. Type 1 and type 2 diabetes are excellent examples of this challenge. While type 1 diabetes leads to high blood glucose levels owing to autoimmune destruction of the insulin-secreting beta cells in the pancreas, type 2 diabetes arises from complex metabolic dysregulation of insulin secretion and the insensitivity of peripheral tissues to the action of insulin, the two are commonly conflated in electronic health records, even for the same patient. This is in part because their corresponding ICD-9 codes are very close to one another (250.01 and 250.02 for type 1 and type 2, respectively), and in part because physicians often lack the data used in research studies to aid in making this distinction: some patients with type 2 diabetes are inevitably classified as type 1 diabetics and, possibly vice versa. This disclaimer regarding diagnostic uncertainty also applies to phenotypes with overlapping clinical signs, such as schizophrenia, schizoaffective and bipolar disorders, and depression, or benign and malignant skin cancers, but does not apply to diseases from radically different biological systems, such as schizophrenia and skin cancer.

URLs. 2010 US Census Urban Area Facts, https://www.census.gov/geo/reference/ua/uafacts.html; ICD-9 codes, https://en.wikipedia.org/wiki/List_of_ICD-9_codes; US Centers for Disease Control and Prevention: Health Insurance, https://www.cdc.gov/nchs/fastats/health-insurance.htm; ACS demographic and housing estimate, https://factfinder.census.gov/faces/tableservices/jsf/pages/productview.xhtml?pid=ACS_15_5YR_DP05&src=pt; US Census Bureau Annual Estimates of the Resident Population: April 1, 2010 to July 1, 2016, https://factfinder.census.gov/faces/tableservices/jsf/pages/productview.xhtml?pid=PEP_2016_PEPANNRES&src=pt; Children by presence and type of parent(s), race, and Hispanic origin: 2007–2011, https://www.census.gov/data/tables/time-series/demo/families/families.html.

METHODS

Methods, including statements of data availability and any associated accession codes and references, are available in the online version of the paper.

Note: Any Supplementary Information and Source Data files are available in the online version of the paper.

AUTHOR CONTRIBUTIONS

All authors contributed extensively to the work presented in this paper. K.W. and A.R. designed experiments, analyzed data, and wrote the manuscript; K.W., H.G., and H.P. performed computational experiments; and N.J.C., H.G., and H.P. contributed to iterative improvement of the manuscript.

COMPETING FINANCIAL INTERESTS

The authors declare no competing financial interests.

Reprints and permissions information is available online at http://www.nature.com/reprints/index.html. Publisher's note: Springer Nature remains neutral with regard to jurisdictional claims in published maps and institutional affiliations.

1. van de Water, T., Suliman, S. & Seedat, S. Gender and cultural issues in psychiatric nosological classification systems. *CNS Spectr.* **21**, 334–340 (2016).
2. Kendler, K.S. The nature of psychiatric disorders. *World Psychiatry* **15**, 5–12 (2016).
3. Endlicher, S. *Genera Plantarum Secundum Ordines Naturales Disposita* (F. Beck, 1836).
4. Jussieu, A.L.d. & Stafleu, F.A. *Genera Plantarum* (Upsaliæ:apud. J. Cramer; Stechert-Hafner Service Agency, 1964).
5. Linné, C.v. *et al. The Families of Plants: With Their Natural Characters, According to the Number, Figure, Situation, and Proportion of All of the Parts of Fructification* (John Jackson, 1787).
6. Thunberg, K.P. *et al. Nova Genera Plantarum* (Upsaliæ :apud. J. Edman etc., 1781).
7. Anderson, M.J. *Carl Linnaeus: Genius of Classification* (Enslow Publishers, 2015).
8. Felsenstein, J. *Inferring Phylogenies* (Sinauer Associates, 2004).
9. Suthram, S. *et al.* Network-based elucidation of human disease similarities reveals common functional modules enriched for pluripotent drug targets. *PLoS Comput. Biol.* **6**, e1000662 (2010).
10. Fisher, R.A. XV.—the correlation between relatives on the supposition of Mendelian inheritance. *Trans. R. Soc. Edinb.* **52**, 399–433 (1918).
11. Wright, S. Systems of mating. I. The biometric relations between parent and offspring. *Genetics* **6**, 111–123 (1921).
12. Lynch, M. & Walsh, B. *Genetics and Analysis of Quantitative Traits* (Sinauer, 1998).
13. Gelman, A. *Bayesian Data Analysis* 3rd edn. (CRC Press, 2014).
14. Hadfield, J.D. MCMC methods for multi-response generalized linear mixed models: the MCMCglmm R package. *J. Stat. Softw.* **33**, 1–22 (2010).
15. Benjamini, Y. & Hochberg, Y. Controlling the false discovery rate—a practical and powerful approach to multiple testing. *J. Royal Stat. Soc. B Met.* **57**, 289–300 (1995).
16. Lichtenstein, P. *et al.* Common genetic determinants of schizophrenia and bipolar disorder in Swedish families: a population-based study. *Lancet* **373**, 234–239 (2009).
17. Boyle, E.A., Li, Y.I. & Pritchard, J.K. An expanded view of complex traits: from polygenic to omnigenic. *Cell* **169**, 1177–1186 (2017).
18. Saitou, N. & Nei, M. The neighbor-joining method: a new method for reconstructing phylogenetic trees. *Mol. Biol. Evol.* **4**, 406–425 (1987).
19. Efron, B. *The Jackknife, the Bootstrap and Other Resampling Plans* (Society for Industrial and Applied Mathematics, 1982).
20. Felsenstein, J. Confidence limits on phylogenies: an approach using the bootstrap. *Evolution* **39**, 783–791 (1985).
21. Efron, B. The bootstrap and Markov-chain Monte Carlo. *J. Biopharm. Stat.* **21**, 1052–1062 (2011).
22. Farh, K.K. *et al.* Genetic and epigenetic fine mapping of causal autoimmune disease variants. *Nature* **518**, 337–343 (2015).
23. Gormley, P. *et al.* Meta-analysis of 375,000 individuals identifies 38 susceptibility loci for migraine. *Nat. Genet.* **48**, 856–866 (2016).
24. Bulik-Sullivan, B. *et al.* An atlas of genetic correlations across human diseases and traits. *Nat. Genet.* **47**, 1236–1241 (2015).
25. Xia, C. *et al.* Pedigree- and SNP-associated genetics and recent environment are the major contributors to anthropometric and cardiometabolic trait variation. *PLoS Genet.* **12**, e1005804 (2016).
26. Schildkraut, J.M., Risch, N. & Thompson, W.D. Evaluating genetic association among ovarian, breast, and endometrial cancer: evidence for a breast/ovarian cancer relationship. *Am. J. Hum. Genet.* **45**, 521–529 (1989).
27. Davis, L.K. *et al.* Partitioning the heritability of Tourette syndrome and obsessive compulsive disorder reveals differences in genetic architecture. *PLoS Genet.* **9**, e1003864 (2013).
28. Lee, S.H. *et al.* Genetic relationship between five psychiatric disorders estimated from genome-wide SNPs. *Nat. Genet.* **45**, 984–994 (2013).
29. Loh, P.R. *et al.* Contrasting genetic architectures of schizophrenia and other complex diseases using fast variance-components analysis. *Nat. Genet.* **47**, 1385–1392 (2015).
30. Muñoz, M. *et al.* Evaluating the contribution of genetics and familial shared environment to common disease using the UK Biobank. *Nat. Genet.* **48**, 980–983 (2016).
31. Vattikuti, S., Guo, J. & Chow, C.C. Heritability and genetic correlations explained by common SNPs for metabolic syndrome traits. *PLoS Genet.* **8**, e1002637 (2012).
32. Liu, C. *et al.* Revisiting heritability accounting for shared environmental effects and maternal inheritance. *Hum. Genet.* **134**, 169–179 (2015).
33. Zuk, O., Hechter, E., Sunyaev, S.R. & Lander, E.S. The mystery of missing heritability: genetic interactions create phantom heritability. *Proc. Natl. Acad. Sci. USA* **109**, 1193–1198 (2012).
34. Zaitlen, N. *et al.* Using extended genealogy to estimate components of heritability for 23 quantitative and dichotomous traits. *PLoS Genet.* **9**, e1003520 (2013).
35. Wray, N.R. & Maier, R. Genetic basis of complex genetic disease: the contribution of disease heterogeneity to missing heritability. *Curr. Epidemiol. Rep.* **1**, 220–227 (2014).
36. Ojodu, J., Hulihan, M.M., Pope, S.N. & Grant, A.M. Incidence of sickle cell trait—United States, 2010. *MMWR Morb. Mortal. Wkly. Rep.* **63**, 1155–1158 (2014).
37. Denny, J.C. *et al.* PheWAS: demonstrating the feasibility of a phenome-wide scan to discover gene–disease associations. *Bioinformatics* **26**, 1205–1210 (2010).

ONLINE METHODS

Data. Our study used data from the 2003–2011 Truven Health MarketScan Commercial Claims and Encounters Database, which comprised 115,805,687 individuals and 56,003,690 policies. We defined a family as a group of individuals on a single insurance policy. In each family, we assumed primary and secondary beneficiaries were parents and other dependents were children.

To maximize the probability of correct genetic relatedness, we selected families with parents and dependents having at least 15 years' age difference. In addition, we set the minimum enrollment time to 6 years, ran our analysis using 128,989 nuclear families with the fullest medical history in our database and which included children aged 16 and above. The resulting 481,657 individuals had been enrolled in the database for an average of 6.5 years.

We grouped ICD-9 diagnostic codes into 568 categories on the basis of their clinical manifestations. We then selected 149 diseases of 20 biological systems for univariate analysis where disease prevalence was larger than 0.3% in parents and children studied, with the standard error calculated as

$$se = \sqrt{\frac{p(1-p)(1-f)}{n}}$$

where n represents the total number of individuals, p is the prevalence, and f is the fraction of the total US population sampled (see URLs). We calculated the age of onset for each disease as the 5% age percentile of all patients with a given disease in the database.

Because all individuals included in this study were between the ages of 17 and 65, several late-onset diseases have lower prevalence. For example, Parkinson's disease prevalence among the parents and their children was 0.28% and 0.024%, respectively (**Supplementary Table 1**). We excluded these diseases with low prevalence in young adults from our study because of insufficient sample size.

We then calculated the phenotypes for each relational pair (parent–offspring, siblings, couples) and selected 29 diseases with at least 30 data points per pairwise disease state and relational category, also belonging to the four biological systems of interest (neuropsychiatric, immune, oncological, and cardiovascular) for bivariate analysis. Because of our focus on the four biological systems listed above and the high computational cost of estimation, several diseases included in the univariate analysis were not included in the bivariate analysis.

Statistical analysis. We used a multivariate, generalized, linear mixed model with a probit link[38], that is, the probability for an individual to have a disease is measured by an underlying Gaussian latent variable (liability ℓ)[39,40]. This model[41] allows us to infer five kinds of factors influencing disease liability variation: genetic effects associated with pedigree, environmental effects shared by couples, environmental effects shared by siblings, environmental effects shared within families, and unique environmental effects. In addition, disease prevalence differed between males and females and between parents and their children. We accounted for these differences in disease liability by including age- and sex-specific fixed effects in our model. We assumed that the same disease manifesting itself both in parents and their children has the same underlying liability, after accounting for age and sex effects.

The outcome vector $\mathbf{y}$ shows a case ($\mathbf{y} = 1$) or control ($\mathbf{y} = 0$) status for each disease on the observed scale. Let liability $\ell = \Phi(\mathbf{y})^{-1}$, where Φ is the cumulative distribution function (CDF) of the standard normal distribution and

$$\ell = \mathbf{X}\beta + \mathbf{a} + \mathbf{c} + \mathbf{s} + \mathbf{f} + \mathbf{e}$$

where β is the vector for fixed effects of age and sex. $\mathbf{a}$ is the vector of random, additive genetic effects based on pedigree, $\mathbf{c}$ is the vector of environmental effects shared by a couple, $\mathbf{s}$ is the vector of environment effects shared by siblings, $\mathbf{f}$ is the vector of environment effects shared by a family, and $\mathbf{e}$ is the vector of unique effects[41]. We followed the naming convention used in Xia *et al.*[25].

The underlying binary traits' liability (co)variance structure[41] is

$$var(\ell) = \mathbf{G} \otimes \mathbf{A} + \mathbf{R}_c \otimes \mathbf{I}_c + \mathbf{R}_s \otimes \mathbf{I}_s + \mathbf{R}_f \otimes \mathbf{I}_f + \mathbf{R}_e \otimes \mathbf{I}_n$$

where $\mathbf{A}$ is the additive genetic relationship matrix (genetic effects are assumed to be additive on the liability scale), $\mathbf{I}_c$ is the couple environment matrix, $\mathbf{I}_s$ is the sibling environment matrix, $\mathbf{I}_f$ is the family environment matrix, $\mathbf{I}_n$ is an identity matrix, $\mathbf{G}$ is the additive genetic (co)variance, $\mathbf{R}_c$ is the couple environment (co)variance, $\mathbf{R}_s$ is the sibling environment (co)variance, $\mathbf{R}_f$ is the family environment (co)variance, and $\mathbf{R}_e$ is the unique environment (co)variance. Furthermore, individual covariance matrices are parameterized as

$$\mathbf{G} = \begin{bmatrix} \sigma_{a,i}^2 & \sigma_{a,i,j} \\ \sigma_{a,i,j} & \sigma_{a,j}^2 \end{bmatrix}, \mathbf{R}_c = \begin{bmatrix} \sigma_{c,i}^2 & \sigma_{c,i,j} \\ \sigma_{c,i,j} & \sigma_{c,j}^2 \end{bmatrix}, \mathbf{R}_s = \begin{bmatrix} \sigma_{s,i}^2 & \sigma_{s,i,j} \\ \sigma_{s,i,j} & \sigma_{s,j}^2 \end{bmatrix},$$

$$\mathbf{R}_f = \begin{bmatrix} \sigma_{f,i}^2 & \sigma_{f,i,j} \\ \sigma_{f,i,j} & \sigma_{f,j}^2 \end{bmatrix}, \mathbf{R}_e = \begin{bmatrix} \sigma_{e,i}^2 & \sigma_{e,i,j} \\ \sigma_{e,i,j} & \sigma_{e,j}^2 \end{bmatrix}$$

The narrow-sense heritability, couple environmental effects, sibling environmental effects, family environmental effects, and unique environmental effects for disease x are defined on the liability scale in the following way

$$h_x^2 = \frac{V_{a,x}}{V_{p,x}}, e_{c,x}^2 = \frac{V_{c,x}}{V_{p,x}}, e_{s,x}^2 = \frac{V_{s,x}}{V_{p,x}}, e_{f,xx}^2 = \frac{V_{f,x}}{V_{p,x}}, e_{u,x}^2 = \frac{V_{u,x}}{V_{p,x}}$$

We calculated the genetic correlation coefficient (r_g) and the environmental correlation coefficient (r_e) as

$$r_g = \frac{\sigma_{a,i,j}}{\sigma_{a,i}\sigma_{a,j}}, r_e = \frac{\sigma_{c,i,j} + \sigma_{s,i,j} + \sigma_{f,i,j} + \sigma_{e,i,j}}{\sqrt{\sigma_{c,i}^2 + \sigma_{s,i}^2 + \sigma_{f,i}^2 + \sigma_{e,i}^2}\sqrt{\sigma_{c,j}^2 + \sigma_{s,j}^2 + \sigma_{f,j}^2 + \sigma_{e,j}^2}}$$

Because of the binary nature of our phenotypic data[42], we estimated variance components using Bayesian methods with the MCMCglmm package[14]. We used a chi-squared prior with 1 d.f. for the univariate analysis[43] and Half–Cauchy prior for the bivariate analyses[44]. For the univariate analyses, we ran a burn-in period of 150,000 to 330,000 iterations depending on convergence and sampled 600,000 iterations with 500 thinning intervals. For bivariate analyses, we ran a burn-in period of 30,000 to 44,000 iterations and sampled 120,000 iterations.

We checked model convergence using both standard MCMC diagnostic tests[45–47] and visual comparison after the burn-in period. We reported parameter estimations with posterior means, posterior s.d., and 95% confidence intervals. The posterior distributions represent the distributions of true parameters, given the data and the priors. Posterior probabilities for sign differences between the same disease genetic and environmental correlations were calculated assuming a bivariate normal posterior distribution. We corrected for multiple testing using the Benjamini–Hochberg method[15,48] and deemed a correlation significant if it passed the false discovery rate of 1%. We also constructed neighbor-joining trees based on a distance definition of 1 – correlation for the correlation matrices[18]. We performed 10,000 simulations for each tree by sampling from the correlation posterior distributions. We calculated a bootstrap-like measure indicating the percentage of simulations that replicated the disease partition.

Model selection. We conducted two rounds of model selection to find the most appropriate genetic and environmental models for both univariate and bivariate analyses using DIC[49]. The full model '*GCSF*', as well as five simpler models, were selected on the basis of 29 diseases involved in both univariate and bivariate analyses. We then conducted a second run of model selection between the top two models on all 149 diseases. Because of the high computational cost of bivariate analysis, we based our bivariate model on univariate model selections and chose the *GCS* model for the bivariate analysis.

Pedigree error. Quantitative genetic estimations, such as those for heritability and genetic correlations, rely on the accuracy of the pedigree information. Intuitively, we expect a downward bias in both heritability and genetic covariance due to pedigree errors. Indeed, simulation and population studies

have shown that heritability estimates were underestimated, albeit slightly; pedigrees with 20% errors led to 5% underestimation of heritability estimates[50,51]. Genetic correlation estimates were influenced even less by misassigned relations: both Morrissey et al.[52] and Bérénos et al.[50] found no biases caused by pedigree errors in genetic correlation estimations using both simulated and real data.

Stepchildren and adopted children. We collected US Census data on children by household type (see URLs)[53]. The 2010 US Census surveyed a large population and reported data for children of differing age groups, shown in **Supplementary Table 7**. **Supplementary Table 8** is based on US Current Population Survey data from 2007 to 2011 for children under the age of 18. These data showed that the percentages of children living with both biological parents were consistent with percentages from US Census data.

Pedigree simulation. Following the simulation model of Charmantier and Réale[51], we performed 100 simulations on 5,000 nuclear families, of which 2.4% have adoptive children and 6.2% have stepchildren[53] and estimated parameters with the true pedigrees versus misassigned pedigrees. We used a stochastic simulation model to generate pedigrees of two generations, with varying heritability estimates (0.03–0.97) and genetic correlations (0.13–0.85). The parents are assumed to be unrelated and unselected individuals. We simulated two binary traits, following the model $y = I (\ell > 0)$, $\ell = \mu + Za + e$ where y is the matrix containing individual phenotypes at both traits, ℓ is the underlying liability, μ contains the population means for liability, a is a matrix of additive genetic effects, and e is a matrix of residual errors. Z represents an incidence matrix of the individual effects a has upon liabilities in ℓ. All models were solved using MCMCglmm. Indeed, we also found a mean underestimation of 5.6% (s.e.m. = 0.56%) for heritability and no evidence of biases for estimations of either genetic (t-test $P = 0.8784$) or environmental (t-test $P = 0.9948$) correlations. We then calculated and reported heritability estimates adjusted for the underestimation.

Heritability comparison. In comparing our heritability estimates with results from other independent studies, we first collected reference family heritability estimates for 65 of the 149 traits we studied. We also collected 31 GWAS heritability estimates from the literature. We reasoned that the two estimates for the same disease agreed with each other when their 95% confidence intervals overlapped. The comparisons are listed in **Supplementary Tables 3** and **6**.

GWAS and family-based genetic correlations. We compared our genetic correlation estimates with estimates using GWAS data on common pairs of traits. First, we collected genetic correlations from literature[24,28,29,54]. Next, we compared those genetic correlation estimates we found in common. To maximize this comparison, we broadened the collection of traits to include non-rheumatic heart disease as a proxy for cardiovascular diseases[29] and type 1 diabetes as a proxy for fasting glucose; see Pippitt et al.[55] for justification of this choice. The 30 resulting genetic correlation pairs (**Supplementary Table 5**) showed a correlation of 0.769, 95% CI = 0.571–0.883 between our estimates and GWAS results, along with a linear fit with a proportionality constant of 1.08 (s.e.m. = 0.167), indicating consistency between the two methods.

Data availability. All data that support the findings of this study are included in this published article (and its supplementary information files). The raw data are available from Truven MarketScan; restrictions apply to the availability of these data, which were used under license for the current study. A user license could be obtained by following the instructions at https://marketscan.truvenhealth.com/marketscanportal/.

38. Korsgaard, I.R. et al. Multivariate Bayesian analysis of Gaussian, right censored Gaussian, ordered categorical and binary traits using Gibbs sampling. *Genet. Sel. Evol.* **35**, 159–183 (2003).
39. Falconer, D. & Mackay, T. *Introduction to Quantitative Genetics* 4th edn. (Longman Scientific and Technical, 1996).
40. Falconer, D.S. The inheritance of liability to certain diseases, estimated from the incidence among relatives. *Ann. Hum. Genet.* **29**, 51–76 (1965).
41. Sorensen, D. & Gianola, D. *Likelihood, Bayesian and MCMC Methods in Quantitative Genetics* (Springer-Verlag, 2002).
42. Rodriguez, G. & Goldman, N. An assessment of estimation procedures for multilevel models with binary responses. *J. R. Stat. S`. Ser. A Stat. Soc.* **158**, 73–89 (1995).
43. de Villemereuil, P., Gimenez, O. & Doligez, B. Comparing parent–offspring regression with frequentist and Bayesian animal models to estimate heritability in wild populations: a simulation study for Gaussian and binary traits. *Methods Ecol. Evol.* **4**, 260–275 (2013).
44. Gelman, A. Prior distributions for variance parameters in hierarchical models (comment on article by Browne and Draper). *Bayesian Anal.* **1**(3), 515–534 (2006).
45. Gelman, A. & Rubin, D.B. Inference from iterative simulation using multiple sequences. *Stat. Sci.* **7**, 457–511 (1992).
46. Heidelberger, P. & Welch, P.D. Simulation run length control in the presence of an initial transient. *Opns Res.* **31**, 1109–1144 (1983).
47. Plummer, M., Best, N., Cowles, K. & Vines, K. CODA: Convergence Diagnosis and Output Analysis for MCMC. *R News* **6**, 7–11 (2006).
48. Benjamini, Y. & Yekutieli, D. The control of the false discovery rate in multiple testing under dependency. *Ann. Stat.* **29**, 1165–1188 (2001).
49. Spiegelhalter, D.J., Best, N.G., Carlin, B.P. & Van Der Linde, A. Bayesian measures of model complexity and fit. *J. Royal Stat. Soc. B Stat. Methodol.* **64**, 583–639 (2002).
50. Bérénos, C., Ellis, P.A., Pilkington, J.G. & Pemberton, J.M. Estimating quantitative genetic parameters in wild populations: a comparison of pedigree and genomic approaches. *Mol. Ecol.* **23**, 3434–3451 (2014).
51. Charmantier, A. & Réale, D. How do misassigned paternities affect the estimation of heritability in the wild? *Mol. Ecol.* **14**, 2839–2850 (2005).
52. Morrissey, M.B., Wilson, A.J., Pemberton, J.M. & Ferguson, M.M. A framework for power and sensitivity analyses for quantitative genetic studies of natural populations, and case studies in Soay sheep (*Ovis aries*). *J. Evol. Biol.* **20**, 2309–2321 (2007).
53. Kreider, R.M. & Lofquist, D.A. Adopted children and stepchildren: 2010. P20-572. (US Census Bureau, 2014).
54. Anttila, V. et al. Analysis of shared heritability in common disorders of the brain. Preprint at *bioRxiv.* https://doi.org/10.1101/048991 (2016).
55. Pippitt, K., Li, M. & Gurgle, H.E. Diabetes mellitus: screening and diagnosis. *Am. Fam. Physician* **93**, 103–109 (2016).